*Int. J. Heat Mass Transfer.* Vol. 26, No. 5, pp. 681–688, 1983
Printed in Great Britain

0017–9310/83/050681–08 $03.00/0
Pergamon Press Ltd.

# THE EFFECT OF THERMAL BOUNDARY CONDITIONS ON THE HEAT TRANSPORT IN VERTICAL CHANNELS HEATED FROM BELOW

H. FRICK*

Kernforschungszentrum Karlsruhe, Institut für Reaktorbauelemente, D-75 Karlsruhe, West Germany, and Department of Earth and Space Sciences, University of California, Los Angeles, CA 90024, U.S.A.

(*Received* 17 *March* 1982)

**Abstract**—A numerical analysis is carried out of the effect of perfectly conducting and adiabatic vertical walls on the heat transport by convection in a fluid heated from below. The equations of motion for a high Prandtl number fluid and the heat equation have been solved by the Galerkin method. Because of the side walls, the convection velocity field has three velocity components and depends on all three spatial coordinates. A two velocity component approximation, as well as the full three component representation of the velocity field, is employed in the numerical analysis. The results indicate the surprising accuracy of the two component approximation. Converged solutions are determined for a range of aspect ratios $A$ between $A = 0$ (Bénard convection) and $A = 20$ (Hele–Shaw convection).

## NOMENCLATURE

$A$, aspect ratio;
$d$, channel width;
$g$, acceleration of gravity;
$k$, channel height;
$\mathbf{j}$, unit vector of the coordinate $y$;
$N$, truncation parameter;
$Nu$, Nusselt number;
$R$, Rayleigh number;
$T_0$, temperature of the lower boundary;
$T_1$, temperature of the upper boundary;
$\Delta T$, temperature difference, $T_0 - T_1$;
$\mathbf{v}$, velocity vector $(u, v, w)$;
$x, y, z$, Cartesian coordinates.

Greek symbols

$\alpha$, wavenumber;
$\gamma$, coefficient of thermal expansion;
$\theta$, temperature;
$\nu$, kinematic viscosity;
$\kappa$, thermal diffusivity.

Subscripts

$c$, critical;
AD, adiabatic;
PC, perfectly conducting.

## 1. INTRODUCTION

ONE OF the most important problems of research on natural convection in fluid layers heated from below is the determination of the heat transport. Cellular convection in a layer of infinite horizontal extent has led to a good understanding of the stability and heat transport over a wide range of Rayleigh numbers [1, 2].

When the convection layer is constrained by vertical walls, the horizontal isotropy is removed and an inhibiting influence on motions in the fluid is exerted by the kinematic and thermal conditions at the side walls. The influence of the side walls on the orientation of the convection rolls in boxes was first theoretically discussed by Davis [3] and experimentally demonstrated by Stork and Müller [4]. While Davis [3] investigated the effect of perfectly conducting walls, Catton [5] studied the effect of adiabatic walls using linear stability theories. Edwards [6] and Catton [7] discussed the influence on the critical Rayleigh number of lateral walls with arbitrary thermal conductivity. The problems of the onset of convection and of finite amplitude convection for the limits of perfectly conducting or adiabatic side walls were treated theoretically by Ostroumov [8] and Yih [9] for an infinite long cylinder and by Charlson and Sani [10, 11] for cylinders with various aspect ratios. In the case of an infinite long channel, Davies-Jones [12] and Frick and Clever [13] have numerically analysed the influence of the side walls on the critical Rayleigh number and the critical wavenumber. The introduction of the aspect ratio $A (A = h/d$, channel height to channel width) made it possible to obtain solutions for a range of aspect ratios between $A = 0$ (Bénard convection) and $A = 100$ (Hele–Shaw convection). Experimental results of the behaviour of convection in closed cells have been presented [14–17]. These investigated the effect of different aspect ratios and of varying the thermal conductivity of the lateral walls. In an experimental investigation of Hele–Shaw convection, Hartline and Lister [18] gave a special definition of the Rayleigh number depending on the full width of a Hele–Shaw box (side walls and gap width) with low conductivity side walls. Koster [19, 20] determined the heat transport in Hele–Shaw experiments for up to four times the critical Rayleigh number using real time holographic interferometry for boxes with approximately adiabatic and perfectly conducting side walls.

The results of the above theoretical and experimental investigations can be summarized as follows. In the presence of side walls, the fluid motion depends on all three spatial coordinates. Owing to the stabilizing

* Present address: Kraftwerk Union, D-605 Offenbach, West Germany.

influence of the lateral walls, the Rayleigh number for the onset of convection increases with increasing aspect ratio $A$. The critical Rayleigh number increases more strongly for perfectly conducting side walls than for adiabatic walls. Conducting walls also reduce the roll size (i.e. increase the wavenumber). The reason for the large increase of the critical Rayleigh number is that the perfectly conducting walls reduce the temperature perturbations in addition to damping the velocity perturbations by viscous dissipation. In the limit of large aspect ratios $A$, the critical Rayleigh number $R_c$ exhibits the relationship $R_c \sim A^2$ for adiabatic side walls and $R_c \sim A^4$ for perfectly conducting side walls. The lateral walls also influence the heat transport. At a fixed value of the Rayleigh number $R > R_c$, the Nusselt number decreases with increasing aspect ratio $A$. For large enough values of $R$, the heat transport increases independently of $A$ and of the thermal boundary conditions at the lateral walls; it is proportional to $R^{0.3}$ as in the case of the 2-dim. Bénard convection [21]. From the stability analysis it is known that the 2-dim. convection rolls in the Bénard case for an infinite Prandtl number fluid become unstable to 3-dim. disturbances at $R_2 = 22\,600$ for all wavenumbers. Here the cross-roll instability and the high Rayleigh number cause a transition to 3-dim. bimodal convection [2]. For high aspect ratios this instability will be suppressed. In the case of adiabatic side walls, the motion is purely 2-dim. owing to the geometry and the lateral boundary conditions. The stability analysis of nonlinear convection in a Hele–Shaw cell with adiabatic side walls by Kvernvold [22] shows that the region of stable convection is limited by the Eckhaus instability and the oscillatory instability. In the case of perfectly conducting side walls, the oscillatory instability was not observed [19]. For an aspect ratio of order unity or lower, the transition to bimodal convection must be expected at high Rayleigh number of the order $R_2$ or higher for both cases of thermal boundary conditions.

This paper represents numerical solutions determined on the basis of a 2-dim. approximation, as well as the full 3-dim. representation of the velocity field, in order to investigate the influence of thermal boundaries and of the aspect ratio of a long horizontal channel on the steady heat transport. The formulation of the basic equations and the numerical method is described in Section 2. In Section 3 the results of the calculations are presented and discussed. This paper represents a major extension of earlier works [13, 21].

## 2. THE GOVERNING EQUATIONS AND THE METHOD OF SOLUTION

We consider a fluid channel heated from below, of height $h$ with infinite extent in the horizontal $x$-direction, and with parallel side walls a distance $d$ apart. The side walls are normal to the $y$-coordinate as shown in Fig. 1. The theoretical description of steady convection in a large Prandtl number fluid is based on

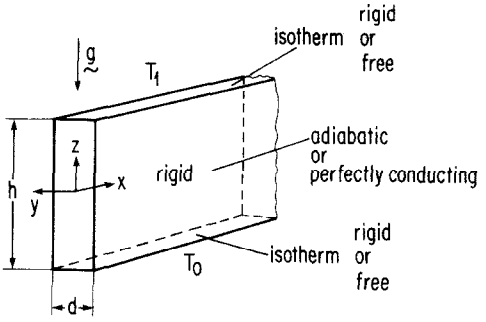


FIG. 1. Geometry and coordinate system.

the Oberbeck–Boussinesq equations. It is convenient to eliminate the equation of continuity by introducing the following general representation for the solenoidal velocity field:

$$\mathbf{v} = \delta\phi + \varepsilon\psi \tag{1}$$

where the operators $\delta$ and $\varepsilon$ are defined by

$$\delta\phi = \nabla \times (\nabla \times \mathbf{j}\phi), \tag{2}$$

$$\varepsilon\psi = \nabla \times (\mathbf{j}\psi). \tag{3}$$

$\mathbf{j}$ denotes the unit vector of the coordinate $y$. The representation (1) is called the three component case in the following. The use of a simplified representation for $\mathbf{v}$

$$\mathbf{v} = \varepsilon\psi \tag{4}$$

has been introduced by Davis [3] and Catton [7] in order to solve the linear problem. Expression (4) describes convection rolls lying in the $y$-direction. Davies-Jones [12] and Frick and Clever [13] have compared solutions obtained by using the representations (1) and (4) for the onset of convection in channels with free and rigid horizontal boundaries and several aspect ratios. Their results show that in a channel with either perfectly conducting or adiabatic side walls the critical Rayleigh number is lower when the general representation (1) is used. The difference in the critical Rayleigh number is at most a few percent for $A \approx 0.5$ and decreases strongly with increasing $A$. In this paper most results are based on approximation (4) which will be referred to as the two component case. Representation (1) is used for selected values of the aspect ratio for comparison.

By introducing dimensionless quantities $h$, $h^2/\kappa$ and $\Delta T/R$ for length, time and temperature and after operating with $\mathbf{j}\cdot\nabla\times(\nabla\times)$ and $\mathbf{j}\cdot\nabla\times$ on the equation of motion, the following equations for the steady variables $\phi$, $\psi$ and $\theta$ are obtained in the limit of large Prandtl number:

$$\nabla^4\Delta_2\phi + A\,\partial^2_{yz}\theta = 0, \tag{5}$$

$$\nabla^2\Delta_2\psi + \partial_x\theta = 0, \tag{6}$$

$$\nabla^2\theta + R(A\,\partial^2_{xy}\phi + \partial_x\psi) = (A\,\partial^2_{xy}\phi - \partial_z\psi)\,\partial_x\theta - A\Delta_2\phi\,\partial_y\theta + (A\,\partial^2_{yz}\phi + \partial_x\psi)\,\partial_z\theta, \tag{7}$$

where $\theta$ is the deviation from the temperature distribution of the static state. $\Delta_2$ denotes the Laplacian with respect to the $x, z$ plane

$$\Delta_2 = \partial_{xx}^2 + \partial_{zz}^2. \tag{8}$$

The Laplacian $\nabla^2$ is defined by

$$\nabla^2 = \partial_{xx}^2 + A^2\,\partial_{yy}^2 + \partial_{zz}^2. \tag{9}$$

A stretched $y$-coordinate has been used such that the side walls are located at $y = \pm\frac{1}{2}$. The dependence of the problem on the physical conditions of the fluid layers has been reduced to two dimensionless parameters: the Rayleigh number $R$ and the aspect ratio $A$. These parameters are defined by

$$R = \frac{\gamma g \Delta T h^3}{\nu\kappa}$$

and (10)

$$A = h/d$$

where $\gamma$ is the coefficient of thermal expansion, $g$ is the acceleration due to gravity, $\Delta T$ is the temperature difference between the lower and upper boundary of the channel, $\nu$ is the kinematic viscosity and $\kappa$ is the thermal diffusivity. Equations (5)–(7) represent a set of partial differential equations for the scalar variables $\phi, \psi$ and $\theta$. In addition to the coupling of the variables $\phi$ and $\psi$ through the differential equations in the case of rigid horizontal boundaries, this coupling occurs also in the boundary conditions as long as both $\phi$ and $\psi$ are present [13]. It is possible, in the case of stress-free top and bottom boundaries, to separate the boundary conditions for $\phi$ and $\psi$. The boundary conditions at the free boundaries of the layer are given by

$$\partial_z\phi = \partial_{zzz}^3\phi = \psi = \partial_{zz}^2\psi = \theta = 0 \quad \text{at } z = \pm\tfrac{1}{2}. \tag{11}$$

At the vertical boundaries the conditions are given by

$$\left.\begin{aligned} &\phi = \partial_y\phi = \psi = 0 \\ &\partial_y\theta = 0 \quad \text{or} \quad \theta = 0 \end{aligned}\right\} \text{at } y = \pm\tfrac{1}{2} \tag{12, 13}$$

where rigid and either adiabatic or perfectly conducting walls are assumed.

When the simplified expression (4) in v is used, where $\phi$ is absent, the set of the partial differential equations (5)–(7) is simplified to

$$\nabla^2\Delta_2\psi + \partial_x\theta = 0, \tag{14}$$

$$\nabla^2\theta + R\,\partial_x\psi = -\partial_z\psi\,\partial_x\theta + \partial_x\psi\,\partial_z\theta \tag{15}$$

where the scalar fields $\psi$ and $\theta$ depend on all three spatial coordinates. Using this approximation it is possible to determine the heat transport in a channel with free as well as rigid top and bottom boundaries. The boundary conditions for $\psi$ in the case of free boundaries are given in equation (11). In the case of rigid walls they are given by

$$\psi = \partial_z\psi = 0 \quad \text{at } z = \pm\tfrac{1}{2}. \tag{16}$$

The equations (5)–(7), (14) and (15) are solved numerically by a Galerkin technique. For this purpose the variables $\phi, \psi$ and $\theta$ are expanded in terms of a series sum of orthogonal functions which satisfy the boundary conditions on $\phi$, $\psi$ and $\theta$,

$$\phi = \sum_{\lambda\nu\beta} a_{\lambda\nu\beta}\,e^{i\lambda\alpha x}\,h_\nu^y(y)h_\beta^z(z) \equiv \sum_{\lambda\nu\beta} a_{\lambda\nu\beta}\phi_{\lambda\nu\beta}, \tag{17}$$

$$\psi = \sum_{\lambda\nu\beta} ib_{\lambda\nu\beta}\,e^{i\lambda\alpha x}\,k_\nu^y(y)k_\beta^z(z) \equiv \sum_{\lambda\nu\beta} ib_{\lambda\nu\beta}\psi_{\lambda\nu\beta}, \tag{18}$$

$$\Theta = \sum_{\lambda\nu\beta} c_{\lambda\nu\beta}\,e^{i\lambda\alpha x}\,l_\nu^y(y)l_\beta^z(z) \equiv \sum_{\lambda\nu\beta} c_{\lambda\nu\beta}\theta_{\lambda\nu\beta}. \tag{19}$$

The various trial functions in equations (17)–(19) are given for different boundary conditions in the Appendix. In the Galerkin method the expressions (17)–(19) are substituted into equations (5)–(7) multiplied by $\phi_{\kappa\mu\gamma}$, $\psi_{\kappa\mu\gamma}$ and $\theta_{\kappa\mu\gamma}$, respectively, and averaged over the fluid layer. Thus a set of algebraic equations for the unknowns $a_{\lambda\nu\beta}$, $b_{\lambda\nu\beta}$ and $c_{\lambda\nu\beta}$ is obtained. In order to compute these coefficients, it is necessary to truncate the representations (17)–(19) at a sufficiently high level. Following the methods described in refs. [25, 24, 13, 21], a truncation parameter $N$ is introduced, such that all coefficients with

$$\lambda + \nu + \beta > N \tag{20}$$

are neglected. A further simplification is possible in that only coefficients with even values of $\lambda + \beta$ are retained [25, 13]. For a given $N$ the set of algebraic equations are solved by a Newton–Raphson iteration procedure for various values of $R$, $A$ and $\alpha$. To determine the value of the truncation parameter, $N$, we follow Denny and Clever [24] by assuming that the solution is sufficiently accurate if the convective heat transfer in terms of the Nusselt number

$$Nu = 1 - 1/R \int_{y=-1/2}^{y=1/2} \int_{x=-\pi/\alpha}^{x=\pi/\alpha} \partial_z\theta|_{z=-1/2}\,dx\,dy \tag{21}$$

changes by less than 1% as $N$ is increased to $N+2$. With the symmetry properties mentioned above, sets of 104, 195 and 328 algebraic equations for the unknowns $b_{\lambda\nu\beta}$ and $c_{\lambda\nu\beta}$ for values of $N = 9, 11$ and 13, respectively are obtained in the two component case. In the three component case the number of algebraic equations for $a_{\lambda\nu\beta}$, $b_{\lambda\nu\beta}$ and $c_{\lambda\nu\beta}$ increases from 204 to 358 as $N$ is changed from 9 to 11.

## 3. RESULTS AND DISCUSSION

In describing the numerical results for steady convection of an infinite Prandtl number fluid in a channel with adiabatic and perfectly conducting lateral walls, we shall concentrate on the convective heat transport for a wide range of Rayleigh numbers $R$ and aspect ratios $A$. The influence of the wavenumber $\alpha$ on the heat transport has been taken into account only as far as $\alpha$ was fixed at the critical wavenumber determined from the linear problem [12, 13] in dependence of the aspect ratio and the thermal lateral boundary conditions. The aspect ratio $A$ varies between the limits $0 \leqslant A \leqslant 20$. Thus we have the opportunity to consider the limiting cases of Bénard convection and Hele–Shaw

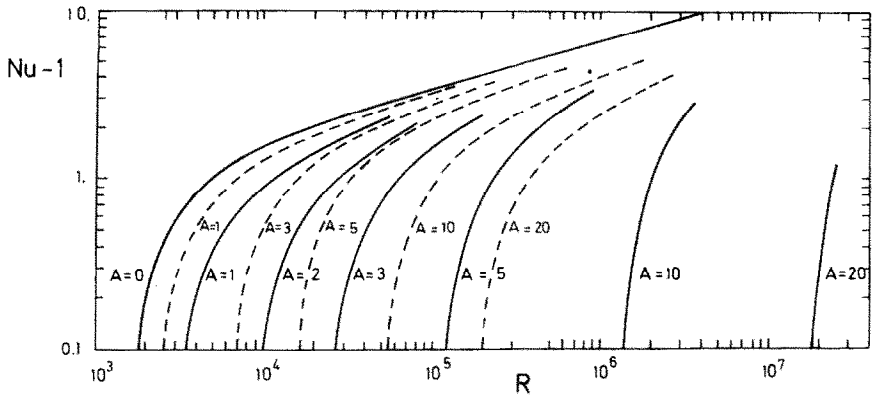


FIG. 2. Heat transport through a confined layer with adiabatic (— — —) and perfectly conducting (————) lateral walls and rigid horizontal boundaries.

convection. In the case $A = 0$, only the horizontal boundaries are important for the behaviour of the convection, but in the case $A \approx 20$ (a thin vertical fluid channel) the side walls impose a rather stringent constraint on the convection flow. The effects of the side walls on the heat transport, on the temperature and on the velocity field are shown in Figs. 2–5. In Figs. 2 and 3 the results for the two component case are shown. Subsequently a comparison of the heat transport values from experiment and theory is shown (Fig. 4) in the case of Hele–Shaw convection. In Fig. 5 the results of the approximate calculations are compared with those for the three component case.

In Fig. 2 the vertical heat transport is displayed in terms of the Nusselt number for both adiabatic and perfectly conducting side walls as a function of the

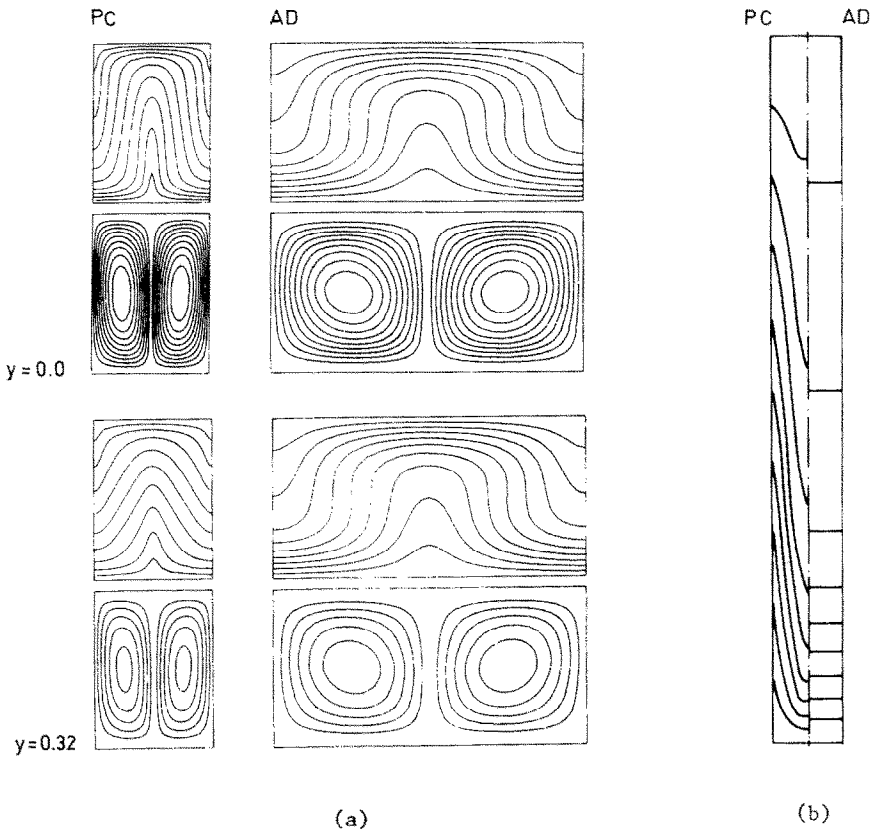


FIG. 3. (a) Temperature field and streamlines in several $y$-planes for $A = 10$, $R = 2R_c$ and $\alpha = \alpha_c$. (b) Isotherms in the zone of downflow along the channel width in the case of the adiabatic (AD) and perfectly conducting (PC) side walls.

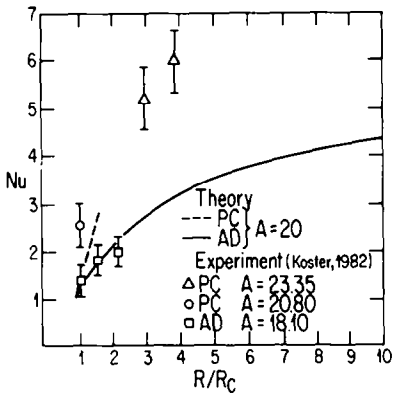


FIG. 4. Comparison of calculated and measured heat transport for Hele–Shaw convection.

Rayleigh number for various aspect ratios. The results in the case of adiabatic side walls are discussed in ref. [21] and are shown here again for comparison with the case of perfectly conducting side walls. As in the case of adiabatic side walls, the different curves of the Nusselt number are bounded from above by the curve for the Bénard problem ($A = 0$). For a fixed value of the aspect ratio $A$, the curves in the case of perfectly conducting side walls always lie under those for the adiabatic case. The curves for both cases climb rapidly with increasing Rayleigh number and approach asymptotically the curve $A = 0$. This is obvious in the case of adiabatic side walls for $A \leqslant 5$ and in the case of perfectly conducting side walls for $A = 1$. Similar results for the slope of Nusselt number curves have been found by Catton and Edwards [14] in their experiments on the heat transfer in hexagonal honeycomb cells. A direct comparison of theoretical and these experimental Nusselt numbers is not possible because of differences in lateral boundary conditions.

The different behaviour of the Nusselt number curves for the two cases of thermal boundary conditions shown in Fig. 2 is mainly due to the different magnitudes of the critical Rayleigh numbers and wavenumbers. In the case of adiabatic side walls the velocity perturbations are damped only through the viscous dissipation. With increasing $A$ the influence of the side walls increases and the critical Rayleigh number and wavenumber increase correspondingly. For perfectly conducting side walls the temperature disturbances are also constrained. From asymptotic considerations it is possible to determine the critical Rayleigh number and wavenumber in the limit of large $A$. In the case of adiabatic side walls $R_c \approx 12(4\pi^2)A^2$ and $\alpha_c = \pi$ are obtained [23] and in the case of perfectly conducting side walls $R_c \approx \pi^4 A^2(A+1)^2$ and $\alpha_c \approx \pi(A^{1/2})$ are found.

In order to demonstrate the effect of lateral boundaries on the convective motion, the distribution of the temperature and velocity in two cross sections is shown in Fig. 3. For adiabatic and perfectly conducting side walls, the temperature and velocity fields have been calculated for the critical wavenumber at twice the initial value of the Rayleigh number. The large difference between the Nusselt numbers ($Nu_{AD} = 2.1$ and $Nu_{PC} = 2.93$) indicates that the nonlinear properties of convection are not influenced as much by the constraints of the side walls as the linear properties. Although the onset of convection is much delayed by the more strongly inhibiting thermally conducting side walls, the growth of the convection amplitude is not inhibited at the same rate. The form of the streamlines differs mainly because of the different critical wavenumber. Owing to the no-slip condition ($\psi = 0$) at the side walls and because of the small width relative to the large height of the channel, the streamlines are strongly dependent on the $y$-coordinate direction. The influence of the thermal boundary conditions on the distribution of the isotherms becomes clearest in Fig. 3. In addition to the temperature field calculated at the planes $y = 0.0$ and $y = 0.32$, the isotherms are shown as a function of $y$ and $z$ in the zone of downflow for both

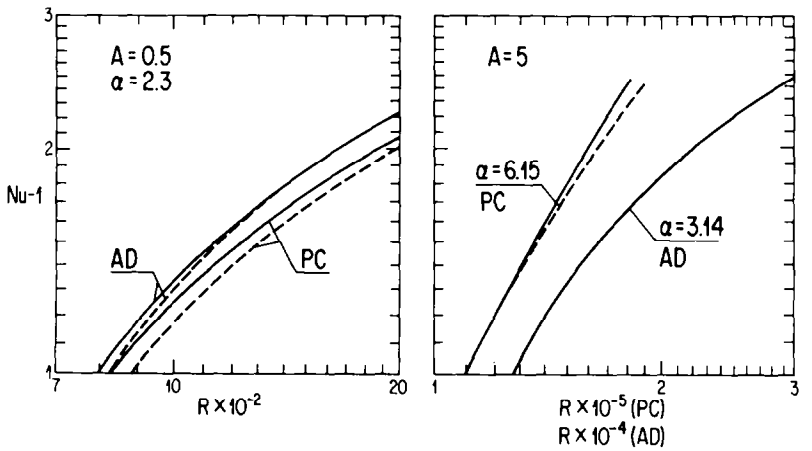


FIG. 5. Nusselt number as a function of Rayleigh number for various values of aspect ratios (given on curves) for a channel with horizontal free boundaries. The solid lines indicate the three velocity component case and the dashed lines indicate the two velocity component case.

cases of the thermal boundary conditions. In the case of adiabatic side walls, the temperature profile is uniform along the channel width in contrast to the case of perfectly conducting side walls where the isotherms are strongly bent across the channel in the flow direction. This dependence of the temperature profile on the thermal boundary condition at the side walls indicates the strong influence of thermal boundary conditions on the convection flow, as shown in the interferometric visualization studies by Koster [20].

A comparison of the Hele–Shaw results ($A = 20$) of the present investigation with experimental results [20] for both thermal limit cases is given in Fig. 4. For $A < 10$ the results for the adiabatic case from theory and experiments have been already discussed in a previous work [21]. In Hele–Shaw experiments, Koster [20] used a Plexiglas box filled with water, which approximates the adiabatic boundary conditions, while a silicone oil filled box with crystal glass walls also used by Koster approximates the perfectly conducting case. For both thermal cases good agreement is found between theory and experiment. Due to numerical convergence difficulties in the case of perfectly conducting side walls, the heat transport could only be calculated in the neighbourhood of the onset of convection. In order to get accurate converged solutions, a truncation parameter $N \geqslant 15$ is necessary for $R/R_c \geqslant 1.33$. The results discussed above have been obtained on the basis of the two-component approximation, equation (4). In Fig. 5, the heat transport determined from calculations using the general representation (1) is compared with results for two component case for a channel with horizontal free boundaries. It is known [12, 13] that the solutions obtained by using the general representation (1) yield lower values of the critical Rayleigh number $R_c$ than those obtained using equation (4). The largest difference in $R_c$ occurs for $A = 0.5$ and decreases rapidly with increasing $A$. In Fig. 5, the heat transport is plotted for $A = 0.5$ (a wide channel) and $A = 5$ (a narrow channel) for both cases of the thermal side walls conditions. The results are obtained for the critical wavenumber. For $A = 0.5$ and adiabatic side walls, the Nusselt number determined by the two component approximation rapidly approaches the results of the fully 3-dim. calculations with increasing Rayleigh number. With increasing aspect ratio, the difference in Nusselt number disappears for adiabatic walls as it is evident from the results for $A = 5$. For perfectly conducting side walls this behaviour is different. For $A = 0.5$, the Nusselt number curves approach each other only slightly within the range of Rayleigh number considered. Another situation occurs for $A = 5$. The difference in the Nusselt number increases with increasing $R$. The reason for this is not clear. However, it does demonstrate the importance of the third velocity component, at least at $A = 5$ in the perfectly conducting case. The similar discrepancy between the two cases is found when $A$ is increased to $A = 10$ and $A = 20$. The enormous computation costs prohibit a more thorough investigation of this phenomenon. Since the difference is relatively small for adiabatic side walls, we conclude that the two component case provides a good approximation of 3-dim. solution in all ranges of parameter space in the adiabatic case.

## 4. CONCLUSION

The Galerkin method has been applied to the problem of finite amplitude convection in a channel heated from below. The influence of perfectly conducting and adiabatic lateral walls on the heat transport has been investigated for several aspect ratios. A two component approximation, as well as the full three component representation, of the velocity field has been employed in the numerical analysis. In the presence of side walls, strictly 2-dim. convection rolls, depending on all three coordinates, must be regarded as an approximation because of the generation of a component of vertical vorticity caused by the temperature gradient parallel to the axis of the rolls. A comparison of the heat transport of the approximate calculations with those obtained by using a general representation for the velocity field has shown that the two component case provides a good approximation to the 3-dim. solution. An unresolved problem in the present investigation is the behaviour of the convection for high Rayleigh number in the case of perfectly conducting side walls and large aspect ratios. This problem is caused by the necessarily large truncation parameter in the Galerkin expansions. There is a question of whether the relatively small difference in the Nusselt number between the two and three component cases changes with increasing Rayleigh number. Computations with higher truncation parameters than were used in this study may possibly clarify this point although this would require enormous amounts of computer time.

The main conclusions are: The curves of the Nusselt number versus the Rayleigh number start off with a relatively steep slope. For a given aspect ratio the heat transport curve for perfectly conducting side walls always lies below the curve for the adiabatic case. For high enough Rayleigh numbers the $Nu$ curves for both adiabatic and perfectly conducting boundary conditions asymptotically approach the heat transport, curve for Bénard convection rolls. In this limit of large Rayleigh number we observe that the Nusselt number increases approximately as $R^{0.3}$ and is independent of aspect ratio and thermal boundary conditions.

*Acknowledgements*—The author is grateful to his thesis advisor Professor U. Müller for making this work possible. He also wishes to thank Professor F. H. Busse and Dr R. M. Clever for many helpful discussions and for their assistance in preparing the manuscript. This work was supported by the Deutsche Forschungsgemeinschaft and by the Atmospheric Science Section of the U.S. National Science Foundation.

## REFERENCES

1. S. Chandrasekhar, *Hydrodynamic and Hydromagnetic Stability*. Oxford Clarendon Press, London (1961).

2. F. H. Busse, Non-linear properties of thermal convection, *Rep. Prog. Phys.* **21**, 1929–1967 (1978).
3. S. H. Davis, Convection in a box: Linear theory, *J. Fluid Mech.* **30**, 465–478 (1967).
4. K. Stork and U. Müller, Convection in a box: Experiments, *J. Fluid Mech.* **54**, 599–611 (1972).
5. I. Catton, The effect of insulating vertical walls on the onset of motion in a fluid layer heated from below, *Int. J. Heat Mass Transfer* **15**, 665–672 (1972).
6. D. K. Edwards, Suppression of cellular convection by lateral walls, *J. Heat Transfer* **91**, 145–150 (1969).
7. I. Catton, Effect of wall conducting on the stability of a fluid in a rectangular region heated from below, *J. Heat Transfer* **94**, 446–452 (1972).
8. G. A. Ostroumov, Free convection under conditions of the internal problem, N.A.C.A. Tech. Memo 1407 (1958).
9. C. S. Yih, Thermal stability of viscous fluids, *Q. Appl. Math.* **17**, 25–42 (1959).
10. G. S. Charlson and R. L. Sani, Thermoconvective instability in a bounded cylindrical fluid layer, *Int. J. Heat Mass Transfer* **13**, 1479–1495 (1970).
11. G. S. Charlson and R. L. Sani, Finite amplitude axisymmetric thermoconvective flows in a bounded cylindrical layer of fluid, *J. Fluid Mech.* **71**, 209–229 (1975).
12. R. P. Davies-Jones, Thermal convection in an infinite channel with no slip side walls, *J. Fluid Mech.* **44**, 695–704 (1971).
13. H. Frick and R. M. Clever, Einfluss der Seitenwände auf das Einsetzen der Konvektion in einer horizontalen Flüssigkeitsschicht, *Z. angew. Math. Phys.* **31**, 502–513 (1980).
14. I. Catton and D. K. Edwards, Effects of side walls on natural convection between horizontal plates heated from below, *J. Heat Transfer* **89**, 295–299 (1967).
15. D. K. Edwards, I. N. Arnold and I. Catton, End clearance effects on rectangular honeycomb collectors, *Solar Energy* **18**, 253–257 (1976).
16. D. K. Edwards, I. N. Arnold and P. S. Wu, Correlations for natural convection through high $L/D$ rectangular cells, *J. Heat Transfer* **101**, 741–743 (1979).
17. P. S. Wu and D. K. Edwards, Effect of combined tilt and end clearance upon natural convection in high $L/D$ rectangular honeycomb, *Solar Energy* **25**, 471–475 (1980).
18. P. K. Hartline and C. R. B. Lister, Thermal convection in a Hele–Shaw cell, *J. Fluid Mech.* **79**, 379–391 (1977).
19. J. N. Koster, Freie Konvektion in vertikalen Spalten, Dissertation (KFK Report 3066), University of Karlsruhe (1980).
20. J. N. Koster, Heat transfer in vertical gaps, *Int. J. Heat Mass Transfer* **25**, 426–428 (1982).
21. H. Frick and R. M. Clever, The influence of side walls on finite amplitude convection in a layer heated from below, *J. Fluid Mech.* **144**, 467–480 (1982).
22. O. Kvernvold, On the stability of non-linear convection in a Hele–Shaw cell, *Int. J. Heat Mass Transfer* **22**, 395–400 (1979).
23. H. Frick, Zellularkonvektion in Fluidschichten mit zwei festen seitlichen Berandungen, Dissertation (KFK Report 3109), University of Karlsruhe (1981).
24. V. E. Denny and R. M. Clever, Comparisons of Galerkin and finite difference methods of solving highly nonlinear thermally driven flows, *J. Comps. Phys.* **16**, 271–284 (1974).
25. R. M. Clever and F. H. Busse, Transition to time-dependent convection, *J. Fluid Mech.* **65**, 625–645 (1974).

## APPENDIX

The following trial functions have been used:

in the $y$-direction

$$h_\nu^y(y) = S_\nu(y), \tag{A1}$$

$$k_\nu^y(y) = \cos[(2\nu-1)\pi y], \tag{A2}$$

$$l_\nu^y(y) = \begin{cases} \cos[(2\nu-2)\pi y] & \text{adiabatic side walls,} \\ \sin[\nu\pi(y+0.5)] & \text{perfectly conducting side walls.} \end{cases} \tag{A3}$$

in the $z$-direction

$$h_\beta^z(z) = \cos[\nu\pi(z+\tfrac{1}{2})] \tag{A4}$$

$$k_\beta^z(z) = \begin{cases} \sin[\beta\pi(z+0.5)] \text{ free boundaries} & \text{(A5)} \\ S_{1/2\beta}(z)\ \beta \text{ even, rigid boundaries,} & \text{(A6)} \\ C_{1/2(\beta+1)}(z)\ \beta \text{ odd, rigid boundaries,} & \end{cases}$$

$$l_\beta^z(z) = \sin[\beta\pi(z+0.5)]. \tag{A7}$$

The use of equations (A1) and (A6) for convection problems was introduced by Chandrasekhar [1].

## EFFETS DES CONDITIONS AUX LIMITES THERMIQUES SUR LE TRANSFERT DE CHALEUR DANS DES CAVITÉS CHAUFFEÉS PAR LE BAS

**Résumé** – L'analyse numérique présentée ici montre l'effet des parois verticales conductrices et adiabatiques sur le transfert de chaleur par convection dans un fluide chauffé par le bas. Les équations du movement et de chaleur ont été résolues par la méthode de Galerkin pour un fluide à grand nombre de Prandtl. A cause des parois latérales, le champ des vitesse possède trois composantes qui dépendent des trois coordonées spatiales. Une approximation pour une vitesse à deux composantes ainsi qu'une représentation du champ de vitesse à trois composantes ont été employeés dans l'analyse numérique. L'approximation pour une vitesse à deux composantes s'est révélée très bonne par la précision des resultats. Des solutions convergentes ont été déterminées pour un domaine de l'allongement $A$ allant de $A = 0$ (convection de Bénard) a $A = 20$ (convection de Hele–Shaw).

## EINFLUSS DER THERMISCHEN RANDBEDINGUNGEN AUF DEN WÄRMETRANSPORT IN VERTIKALEN VON UNTEN BEHEIZTEN KANÄLEN

**Zusammenfassung** – Eine numerische Analyse, die den Einfluss von perfekt wärmeleitenden und adiabaten Wänden auf den Wärmetransport infolge von Konvektion in einem von unten beheizten Fluid zeigt, wird vorgestellt. Die Bewegungsgleichungen und die Energiegleichung sind für Fluide mit hoher Prandtlzahl mit

Hilfe des Galerkin-Verfahrens gelöst worden. Infolge der Seitenwände besteht das Geschwindigkeitsfeld aus drei Geschwindigkeitskomponenten und hängt von allen drei Raumkoordinaten ab. Sowohl eine Approximation von zwei Geschwindigkeitskomponenten als auch die volle Darstellung mit drei Komponenten des Geschwindigkeitsfeldes wird für die numerische Analyse verwendet. Die Ergebnisse zeigen eine überraschende Genauigkeit der Zweikomponenten-Approximation. Konvergente Lösungen sind für den Geometrieparameter $A$ von $A = 0$ (Bénard-Konvektion) bis $A = 20$ (Hele–Shaw-Konvektion) bestimmt worden.

## ВЛИЯНИЕ ТЕПЛОВЫХ ГРАНИЧНЫХ УСЛОВИЙ НА ПЕРЕНОС ТЕПЛА В ВЕРТИКАЛЬНЫХ КАНАЛАХ ПРИ НАГРЕВЕ СНИЗУ

**Аннотация**—Численно исследовано влияние идеально проводящих и адиабатических вертикальных стенок на конвективный теплоперенос в жидкости при нагреве снизу. Уравнения движения для жидкости с большим числом Прандтля и уравнение теплопроводности решались методом Галеркина. Из-за влияния боковых стенок конвективное поле скоростей имеет три компоненты и зависит от всех трех пространственных координат. При анализе использовались как двухкомпонентное, так и полное трехкомпонентное представления поля скорости. Результаты свидетельствуют о большой точности двухкомпонентного приближения. Получены сходящиеся решения для отношения сторон (A) в диапазоне от A = 0 (конвекция Бенара) до A = 20 (конвекция Хеле-Шоу).